The unambiguous identification and characterization of the hydrido species required both X-ray and NMR data. The X-ray crystallographic results, as shown in Figure 3, provide an excellent picture of the $[W_3S_4H_3(dmpe)_3]^+$ cation except for its most critical feature, the hydrogen atoms. We are left to infer that they occupy the apparently empty positions in the coordinated spheres of the tungsten atoms. The fact that the rest of the cation retains almost identically the same structure as the $[W_3S_4Cl_3(dmpe)_3]^+$ ion leaves no doubt that we are still dealing with $[W_3S_4X_3(dmpe)_3]^+$ ion in which X is a monatomic, uninegative anion that has an extremely small scattering factor for X-rays. Only H^- fits these requirements. Even though the H^- ion (formally speaking) should be a softer, more electron-donating ligand than Cl^-, the W-W distances in the two clusters are identical within the uncertainties. There are some small differences in the W-S and W-P distances, however. Both the Cl and H atoms lie trans to one W-(μ_2-S) bond.

Acknowledgment. We are grateful to both the National Science Foundation and the Robert A. Welch Foundation for financial support. We also thank Professor Zvi Dori of the Technion as well as Drs. Larry R. Falvello and Willi Schwotzer for their interest and assistance.

Supplementary Material Available: Tables of positional parameters, bond lengths, bond angles, and anisotropic displacement parameters for **1-4** and cyclic voltammograms of $[Mo_3S_4Cl_3(dmpe)_3][PBh_4]$ and $[W_3S_4Cl_3(depe)_3][BPh_4]$ (31 pages); tables of observed and calculated structure factors for **1-4** (63 pages). Ordering information is given on any current masthead page.

The Use of Very Crowded Silylamide Ligands $-N(SiMe_nPh_{3-n})_2$ (n = 0, 1, or 2) To Synthesize Crystalline, Two-Coordinate Derivatives of Mn(II), Fe(II), and Co(II) and the Free Ion $[Ph_3SiNSiPh_3]^-$

Hong Chen, Ruth A. Bartlett, H. V. Rasika Dias, Marilyn M. Olmstead, and Philip P. Power*

Contribution from the Department of Chemistry, University of California, Davis, California 95616. *Received November 17, 1988*

Abstract: The synthesis, spectroscopy, and structures of several lithium salts of very bulky silylamides and some of their transition-metal derivatives are described. In addition, the structures of two of the bis(silyl)amine precursors, $HN(SiMePh_2)_2$ and $HN(SiPh_3)_2$, are reported. The lithium derivatives include the monomeric solvates $Li(THF)_2N(SiMePh_2)_2$, **1**, $Li(THF)_2N(SiPh_3)_2$, **2**, and Li(12-crown-4)$N(SiMePh_2)_2$, **3**, and the salt $[Li(12\text{-crown-}4)_2][N(SiPh_3)_2]\cdot THF$, **4**, involving the free $[N(SiPh_3)_2]^-$ ion with a wide SiNSi angle. Four transition-metal derivatives, $M[N(SiMePh_2)_2]_2$ (M = Mn, **5**; Fe, **6**; Co, **7**) and $Fe[N(SiMe_2Ph)_2]_2$, **8**, are also reported. All compounds were characterized by X-ray crystallography, and the transition-metal species were further examined by ^1H NMR, UV-vis, and EPR spectroscopy and magnetic measurements. The transition-metal complexes are all high spin with essentially two coordination and near linear geometries for **5**, **6**, and **8**, whereas **7**, the Co derivative, has an NCoN angle 147.0 (1)° with the possibility of further weak metal ligand interactions that could not be confirmed by ^1H NMR. The structures of the silylamine precursors and the lithium salts **1** to **4** provide evidence of crowding through wide SiNSi angles in the case of the former and monomeric or dissociated structures including wide SiNSi angles for **1-4**. The species **6** and **7**, which were described in a preliminary communication, were the first crystalline, two-coordinate derivatives of iron and cobalt to be reported. In addition, the recently communicated structure of the ion $[Ph_3SiNSiPh_3]^-$ was the first of its kind. It is isoelectronic to $[PPN]^+$ and has short (1.634 Å) Si-N bonds. Crystal data with Mo Kα (λ = 0.71069 Å) radiation at 130 K: $HN(SiMePh_2)_2$, $C_{26}H_{27}NSi_2$, a = 13.683 (4) Å, b = 7.953 (1) Å, c = 22.196 (6) Å, β = 104.12 (2)°, Z = 4, monoclinic, space group $P2_1/n$, R = 0.039; **1**, $C_{34}H_{42}LiNO_2Si_2$, a = 17.675 (4) Å, b = 12.111 (3) Å, c = 15.986 (2) Å, β = 107.89 (1)°, Z = 4, monoclinic, space group $C2/c$, R = 0.044; **2**, $C_{44}H_{46}LiNO_2Si_2$, a = 24.945 (11) Å, b = 10.296 (3) Å, c = 20.658 (9) Å, β = 134.29 (2)°, Z = 4, monoclinic, space group $C2/c$, R = 0.048; **3**, $C_{34}H_{42}LiNO_4Si_2$, a = 11.664 (3) Å, b = 13.971 (6) Å, c = 19.537 (7) Å, Z = 4, orthorhombic, space group $Pbcn$, R = 0.058; **5**, $C_{52}H_{52}MnN_2Si_4$, a = 10.893 (1) Å, b = 15.399 (6) Å, c = 27.049 (4) Å, β = 91.73 (1)°, Z = 4, monoclinic $P2_1/c$, R = 0.040; **8**, $C_{32}H_{44}FeN_2Si_4$, a = 15.137 (5) Å, b = 12.996 (4) Å, c = 17.662 (5) Å, β = 90.85 (2)°, Z =4, monoclinic, space group $P2_1/c$, R = 0.042.

Hexamethyldisilazane, $HN(SiMe_3)_2$, first characterized in 1944,[1] has proved to be an extremely convenient starting material for the synthesis of many hundreds of compounds involving the bulky $-N(SiMe_3)_2$ group.[2] The utility of this ligand in the stabilization of compounds with low coordination numbers or unusual bonding was first recognized in 1963 with the synthesis of several transition-metal derivatives.[3,4] In addition, its alkali metal salts may function as good proton abstractors, and these have found wide use in organic chemistry. However, with the exception of the related $-N(t\text{-Bu})SiMe_3$ ligand[5] and an isolated report[6] on Ge(II), Sn(II), and Pb(II) derivatives of $-N(SiEt_3)_2$ and $-N(GePh_3)_2$ there has been little exploration of the novel coordination which might result from changing the size of the silyl

(1) Sauer, R. O. *J. Am. Chem. Soc.* **1944**, *66*, 1707.
(2) (a) Lappert, M. F.; Power, P. P.; Sanger, A. R.; Srivastava, R. C. *Metal and Metalloid Amides*; Ellis Horwood: Chichester, England, 1980. (b) Bradley, D. C. *Chem. Br.* **1975**, *11*, 393. (c) Eller, P. G.; Bradley, D. C.; Hursthouse, M. B.; Meek, D. W. *Coord. Chem. Rev.* **1977**, *24*, 1. (d) Tilley, T. D.; Andersen, R. A.; Zalkin, A. *Inorg. Chem.* **1984**, *23*, 2271.
(3) Bürger, H.; Wannagat, U. *Monatsh.* **1963**, *94*, 1007.
(4) Bürger, H.; Wannagat, U. *Monatsh.* **1964**, *95*, 1099.
(5) Harris, D. H.; Lappert, M. F. *J. Organomet. Chem. Libr.* **1976**, *2*, 13.
(6) Gynane, M. J. S.; Harris, D. H.; Lappert, M. F.; Power, P. P.; Riviere, P.; Riviere-Baudet, M. *J. Chem. Soc., Dalton Trans.* **1977**, 2004.

0002-7863/89/1511-4338$01.50/0

Table I. Important Bond Distances (Å) and Angles (deg) for Disilylamines

	$HN(SiH_3)_2$[a]	$HN(SiMe_3)_2$[a]	$HN(SiMePh_2)_2$[b]	$HN(SiPh_3)_2$[b]	$HN\{Si(t\text{-}Bu)_3\}_2$[c]
N-Si	1.724 (2)	1.735 (12)	1.720 (2)	1.722 (3)	1.760 (5)
SiNSi	127.9 (2)	125.5 (1.8)	131.6 (1)	136.1 (2)	167 (2)

[a] Reference 18. [b] This work. [c] Reference 19.

substituents. Recent results[7] from this laboratory have shown that the use of more hindered disilazanes has allowed the isolation of the first free amide ion $[Ph_3SiNSiPh_3]^-$ that probably involves significant NSi multiple bonding and a wide Si-N-Si angle of 154.9 (3)°. In addition, it has been shown[8] that the $-N(SiMePh_2)_2$ ligand permits the isolation of the first crystalline, two-coordinate derivatives of the both iron and cobalt as the complexes $M[N(SiMePh_2)_2]_2$ (M = Fe or Co), whereas the only structurally characterized neutral two-coordinate open shell (non d^{10}) transition-metal complexes that had been published involved the manganese compounds $Mn[C(SiMe_3)_3]_2$,[9] $Mn[CH_2t\text{-}Bu]_2$,[10] and $Mn(NMesBMes_2)_2$.[11]

In this paper the synthesis and structural characterization of a range of lithium salts of the ligands $-N(SiMePh_2)_2$ and $-N(SiPh_3)_2$ and their interaction with 12-crown-4 are reported. In addition, the X-ray crystal structures of the amine precursors $HN(SiMePh_2)_2$ and $HN(SiPh_3)_2$ are given. Full details of the synthesis and structures of the two-coordinate transition-metal species $M[N(SiMePh_2)_2]_2$ (M = Mn, Fe, or Co) and $Fe[N(SiMe_2Ph)_2]_2$ along with their characterization by UV-vis, ^1H NMR, EPR, and magnetic measurements are also described.

Experimental Section

General Procedures. All work was performed by using Schlenk techniques under N_2 or a Vacuum Atmospheres HE43-2 drybox. Solvents were freshly distilled under N_2 from Na/K or Na/K benzophenone ketyl and degassed twice immediately before use.

Physical Measurements. ^1H NMR spectra were obtained on General Electric QE-300 or Nicolet NT-360 spectrometers. Isotropic shifts were calculated from the relationship $(\Delta H/H_o)_{iso} = (\Delta H/H_o)_{obsd} - (\Delta H/H_o)_{dia}$ in which the diamagnetic reference shifts are those of the silylamine ligand precursors in C_6D_6 or C_7D_8. Electronic absorption spectra were obtained on a Hewlett-Packard 8450A UV-vis spectrometer. EPR data were obtained on a Brucker ER-200D spectrometer operating at 9.48 G Hz. All compounds gave satisfactory C, H, and N analysis.

Starting Materials. The compounds $HN(SiMe_2Ph)_2$,[12] $HN(SiMePh_2)_2$,[13] $HN(SiPh_3)_2$,[14] and MnI_2[15] were synthesized by literature methods. $CoCl_2$ (Aldrich), $FeBr_2$ (Cerac), and 1.6 M *n*-BuLi in hexane (Aldrich) were purchased from the commercial suppliers and were used without further purifications.

Synthesis of the Lithium Salts 1-4. All the lithium amide salts were synthesized in the first instance by treatment of a hexane/THF solution of the appropriate amine with 1.6 M *n*-BuLi in hexane. In a typical experiment $HN(SiMePh_2)_2$ (1.63 g, 4 mmol) in hexane (20 mL) and THF (2 mL), cooled in an ice bath, was treated dropwise with a 1.6 M hexane solution (2.5 mL) of *n*-BuLi. The reaction was stirred for 1 h and allowed to come to ambient temperature. The volatile components were removed under reduced pressure to incipient crystallization (volume = 5-10 mL). Cooling overnight in a −20 °C freezer gave crystals of 1 in about 70% yield (1.55 g, not optimized): mp 98-100 °C. Compound **2** was synthesized in an identical fashion. The crystals, however, are somewhat less soluble than those of 1: mp 134-137 °C.

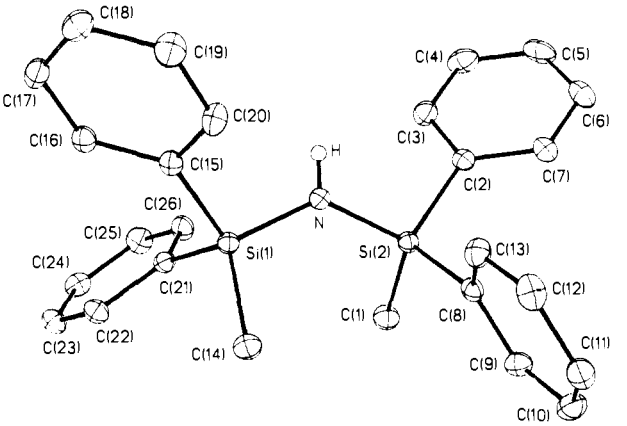

Figure 1. Computer-generated drawing of $HN(SiMePh_2)_2$. Hydrogen atoms omitted for clarity.

Li(12-crown-4)N(SiMePh$_2$)$_2$, 3. The complex **3** was synthesized by the addition of 12-crown-4 (either 1 equiv or excess) to the solution formed from $HN(SiMePh_2)_2$ (1.63 g, 4 mmol), 2.5 mL of a 1.6 M BuLi/hexane solution and hexane (25 mL). After stirring for 1 h, reduction of the volume under reduced pressure to ca. 7 mL gave, upon cooling in a −20 °C freezer overnight, colorless crystals of **3** in 50% yield (1.63 g, not optimized): mp 102-105 °C.

[Li(12-crown-4)$_2$][N(SiPh$_3$)$_2$]·THF, 4. $HN(SiPh_3)_2$ (1.06 g, 2 mmol) in THF (20 mL) was treated dropwise with *n*-BuLi (1.3 mL of a 1.6 M solution in hexane). After 1 h 12-crown-4 (0.7 mL, ~4 mmol) was added by syringe, and the resultant solution was stirred for 10 min. Filtration, followed by a reduction in volume under reduced pressure to incipient crystallization and overnight cooling in a −20 °C freezer gave **4** as colorless crystals: yield 1.1 g, 58%; mp 178-182 °C.

M[N(SiMePh$_2$)$_2$]$_2$ (M = Mn, 5; Fe, 6; Co, 7). The synthesis of each compound was very similar. In a typical experiment $HNSi(MePh_2)_2$ (3.26 g, 8 mmol) in THF (30 mL), cooled in an ice bath, was treated dropwise with *n*-BuLi (5 mL of a 1.6 M hexane solution) and stirred for 1 h. $CoCl_2$ (0.52 g, 4 mmol) was then added via a solid addition tube. The solution was allowed to come to ambient temperature and was stirred for a further 12 h to give a green solution. The volatile components were removed under reduced pressure, and the residue was dissolved in toluene (25 mL) and filtered. The volume of the green solution was halved under reduced pressure, and hexane (~10 mL) was added. Filtration and a slight volume reduction resulted in the appearance of green crystals on the wall of the Schlenk tube. These were redissolved by slight warming. Slow cooling over 24 h in a −20 °C freezer gave the product **7** as dark-green/turquoise dichroic crystals: yield 2.1 g, 60%; mp 147-150 °C (soften at 100 °C). The compounds **5** and **6** were synthesized in a similar yield by the same route using MnI_2 or $FeBr_2$ starting materials. For **5** the crystals were pale pink, mp 157-159 °C dec; for **6** the crystals were pale amber, mp 158-160 °C.

Fe[N(SiMe$_2$Ph)$_2$]$_2$, 8. $HN(SiMe_2Ph)_2$ (2.3 g, 8 mmol) in THF (30 mL), cooled in an ice bath, was treated dropwise with *n*-BuLi (5 mL of 1.6 M solution in hexane). $FeBr_2$ (0.86 g, 4 mmol) was then added. Stirring for 2 h gave a pale brown solution which was allowed to come to room temperature and stirred for a further 2 h. Removal of the volatile components under reduced pressure followed by extraction of the residue in hexane (25 mL) and filtration gave a yellow-brown solution. Reduction of the volume to about 7-8 mL under reduced pressure and cooling in a −20 °C freezer for 2 days gave the product **8** as large straw-colored crystals: yield 0.98 g, 40%; mp 98-104 °C.

X-ray Data Collection, Solutions, and Refinement of the Structures. All X-ray data were collected with use of a Syntex $P2_1$ diffractometer equipped with a graphite monochromator and locally modified LT-1 device for low-temperature work. Crystallographic programs used were those of SHELXTL, Version 5, installed on a Data General Eclipse computer. Scattering factors were from Vol. IV of ref 16. All compounds

(7) Bartlett, R. A.; Power, P. P. *J. Am. Chem. Soc.* **1987**, *109*, 6509.
(8) Bartlett, R. A.; Power, P. P. *J. Am. Chem. Soc.* **1987**, *109*, 7563.
(9) Buttrus, N. H.; Eaborn, P. B.; Hitchcock, P. B.; Smith. J. D.; Sullivan, A. C. *J. Chem. Soc., Chem. Commun.* **1985**, 1380.
(10) Andersen, R. A.; Haaland, A.; Rypdal, K.; Volden, H. V. *J. Chem. Soc., Chem. Commun.* **1985**, 1807.
(11) Bartlett, R. A.; Feng, X.; Olmstead, M. M.; Power, P. P.; Weese, K. J. *J. Am. Chem. Soc.* **1987**, *109*, 4851. Two-coordinate Cr(II) and Ni(II) derivatives of the -NMesBMes$_2$ are also known. Bartlett, R. A.; Chen, H.; Power, P. P. *Angew. Chem., Int. Ed. Engl.*, in press.
(12) Shostakovskii, M. F.; Kondrat'ev, K. I. *Izvest. Akad. Nauk. S.S.S.R., Otdel. Khim. Nauk.* **1956**, 811; *Chem. Abstr.* **1957**, *51*, 3486.
(13) Andrianov, K. A.; Kononov, A. M.; Makanova, N. N. *Zh. Obshch. Khim.* **1966**, *36*, 895.
(14) Reynolds, H. H.; Bigelow, L. A.; Kraus, C. A. *J. Am. Chem. Soc.* **1929**, *51*, 3071.
(15) Normant, J. F.; Cahiez, G. In *Modern Synthetic Methods*; Scheffold, R., Ed.; Salle and Savenlander: Frankfurt, 1983; Vol. 3.
(16) *International Tables for X-ray Crystallography*; Kynoch Press: Birmingham, England, 1974; Vol. IV.

Table II. Important Bond Distances (Å) and Angles (deg) for Lithium Salts of $-N(SiR_3)_2$ Ligands

	Li(12-crown-4)N(SiMe$_3$)$_2$[a]	Li(THF)$_2$N(SiMePh$_2$)$_2$ (1)	Li(THF)$_2$N(SiPh$_3$)$_2$ (2)	Li(12-crown-4)N(SiMePh$_2$)$_2$ (3)	[Ph$_3$SiNSiPh$_3$]$^-$ (4)
Li–N	1.965 (4)	1.949 (6)	1.998 (7)	2.064 (14)	
N–Si	1.681 (2)	1.671 (1)	1.666 (1)	1.667 (3)	1.633 (4)
					1.634 (4)
Li–O	2.094 (4)	1.907 (3)	1.945 (4)	2.173 (7)	
	2.107 (4)			2.229 (7)	
	2.393 (4)				
	2.332 (4)				
SiNSi	123.5 (1)	132.3 (1)	140.5 (2)	133.9 (4)	154.9 (3)
OLiO	116.2 (2)	111.6 (3)	101.4 (3)	120.5 (6)	
	123.5 (2)			123.1 (6)	

[a] Reference 20.

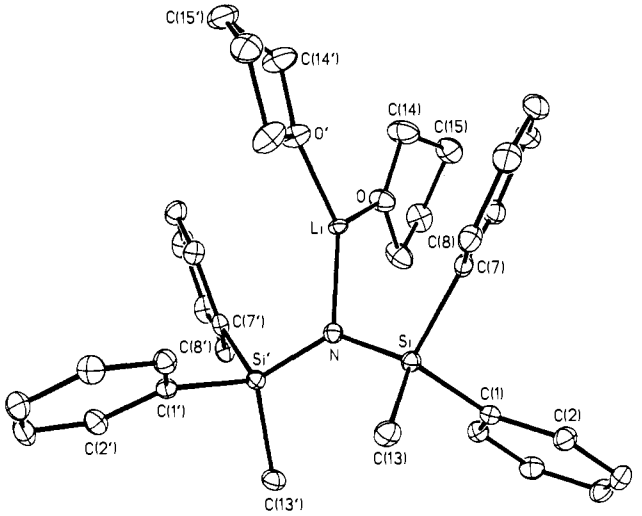

Figure 2. Computer-generated drawing of 1. Hydrogen atoms omitted for clarity.

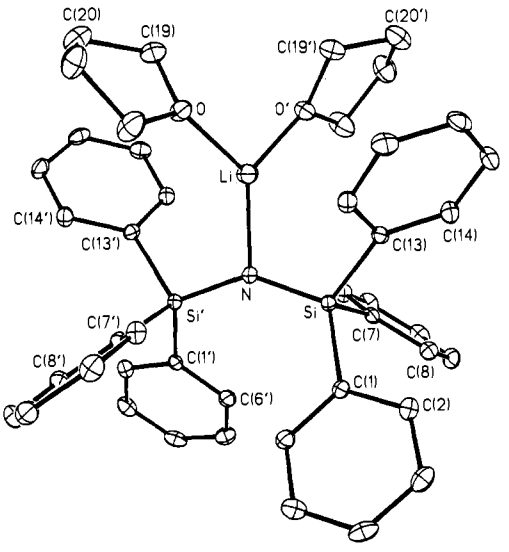

Figure 3. Computer-generated drawing of **2**. Hydrogen atoms omitted for clarity.

were coated with a layer of hydrocarbon oil upon removal from the Schlenk tube. A suitable crystal was selected, attached to a glass fiber by silicone grease, and immediately placed in the low-temperature N_2 stream.[17] The crystal data and refinement for the compounds HN(SiMe$_2$Ph)$_2$ 1, **2**, **3**, **5**, and **8**, are described in Table S1 of the Supplementary Material. Crystal data and some structural data for HN(SiPh$_3$)$_2$, **4**, **6**, and **7**, have been published in preliminary communications. Their structures are also discussed here both for completeness and in order to place them in context with respect to the unreported compounds above.

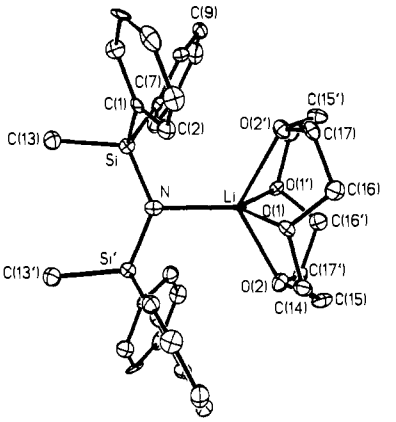

Figure 4. Computer-generated drawing of **3**. Hydrogen atoms omitted for clarity.

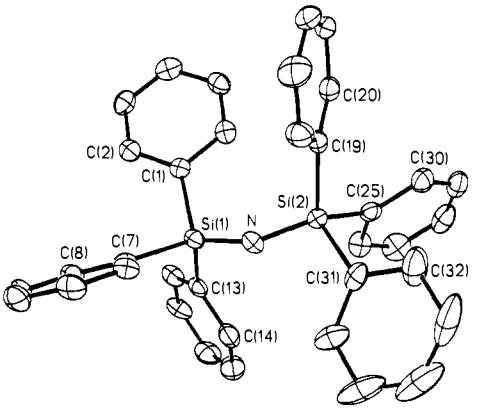

Figure 5. Computer-generated drawing of the anion of **4**. Hydrogen atoms omitted for clarity.

Results and Discussion

Structural Descriptions. HN(SiMePh$_2$)$_2$ and HN(SiPh$_3$)$_2$. Both structures consist of well-separated molecules. A molecule of HN(SiMePh$_2$)$_2$ is illustrated in Figure 1. The structure of HN(SiPh$_3$)$_2$ was illustrated in a preliminary publication.[8] The nitrogen centers are planar in each case. The most important features of the structures involve wide NSiN angles of 131.6 (1)° for HN(SiMePh$_2$)$_2$ and 136.1 (2)° for HN(SiPh$_3$)$_2$. The average N–Si distance in both molecules is near to 1.72 Å. For comparison purposes the important details are provided in Table I along with similar data for other disilylamines.[18,19]

(17) Hope, H. *ACS Symposium Series No. 357*; American Chemical Society: Washington, DC, Wayda, A. L., Darensbourg, M. Y., Eds.; Chapter 10, p 257.

(18) Robiette, A. G.; Sheldrick, G. M.; Sheldrick, W. S.; Beagley, B.; Cruickshank, D. W.; Monaghan, J. J.; Aylett, B. J.; Ellis, I. A. *J. Chem. Soc., Chem. Commun.* **1968**, 909.

(19) Wiberg, N.; Kühnel, E.; Schurz, K.; Bormann, H.; Simon, A. *Z. Naturforsch.* **1988**, *43B*, 1075.

Table III. Important Bond Distances (Å) and Angles (deg) for Two-Coordinate Transition-Metal Amides

	$M[N(SiMePh_2)_2]_2$			$Fe[N(SiMe_2Ph)_2]_2$
M	Mn(5)	Fe(6)	Co(7)	Fe(8)
M-N(1)	1.989 (3)	1.916 (2)	1.898 (3)	1.896 (2)
M-N(2)	1.988 (3)	1.918 (2)	1.904 (3)	1.909 (2)
N-Si(1)	1.719 (3)	1.722 (2)	1.718 (4)	1.713 (2)
N-Si(2)	1.706 (3)	1.713 (2)	1.725 (4)	1.716 (2)
N-Si(3)	1.708 (3)	1.715 (2)	1.710 (3)	1.716 (2)
N-Si(4)	1.716 (3)	1.717 (2)	1.716 (3)	1.705 (2)
M···C	2.774 (5), C(7)	2.695 (4), C(14)	2.584 (7), C(27) 2.588 (7), C(7)	2.633, C(3)
N-M-N	170.7 (1)	169.0 (1)	147.0 (1)	172.1 (1)
Si-N(1)-Si	127.7 (2)	131.8 (1)	125.5 (2)	126.7 (1)
Si-N(2)-Si	131.8 (2)	127.1 (2)	126.7 (2)	127.7 (1)
M-N-Si(1)	107.5 (1)	121.9 (1)	103.4 (2) (av)	113.6 (1) (av)
M-N-Si(2)	120.6 (1)	106.1 (1)	130.5 (2) (av)	119.3 (1) (av)
M-N-Si(3)	116.7 (1)	117.8 (1)		
M-N-Si(4)	115.4 (1)	115.0 (1)		

Vapor Electron Diffraction Data[a] for the Linear Monomers $M[N(SiMe_3)_2]_2$

M	Mn	Fe	Co
M-N	1.95 (2)	1.84 (2)	1.84 (2)

[a] Reference 25.

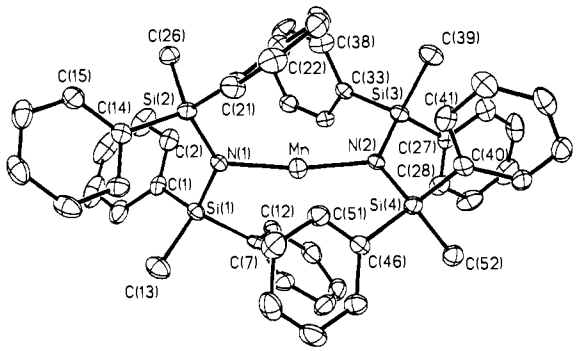

Figure 6. Computer-generated drawing of **5**. Hydrogen atoms omitted for clarity.

$Li(THF)_2N(SiMePh_2)_2$ (1), $Li(THF)_2N(SiPh_3)_2$ (2), Li(12-crown-4)$N(SiMePh_2)_2$ (3), and $[Li(12\text{-crown-4})_2][N(SiPh_3)_2]\cdot THF$ (4). The structures of **1**, **2**, **3**, and **4** (anion) are illustrated in Figures 2–5. The structure of **4** was also illustrated in a preliminary publication[7] but owing to its unique features is also reproduced here. Important structural data for all complexes and, in addition, data for Li(12-crown-4)$N(SiMe_3)_2$[20] are provided in Table II. From the figures it can be seen that the structures of the solvated species **1** and **2** are monomeric. In addition, they are well-separated in the crystal with no close intermolecular contacts. The structure of **3** is similar to that of Li(12-crown-4)$N(SiMe_3)_2$ with some variations in the Li–N and Li–O distances. In the case of **4** cation–anion separation has been achieved to give the ions $[Li(12\text{-crown-4})_2]^+$ and $[N(SiPh_3)_2]^-$. One molecule of THF per ion pair is also present in this structure. The species of **1–3** are characterized by 2-fold rotation axes along the Li–N bonds which implies planarity at the nitrogen centers and the lithium centers in **1** and **2**. In additon **1–4** display short N–Si bonds and wide N–Si–N angles. This is especially true of the ion $[N(SiPh_3)_2]^-$ (Table II). The Li–N distances range from about 1.95 to 2.06 Å. The Li–O bonds show significantly greater variation of between 1.907 and 2.229 Å.

$M[N(SiMePh_2)_2]_2$ (M = Mn, 5; Fe, 6; and Co, 7) and $Fe[N(SiMe_2Ph)_2]_2$, 8. View of **5**, **7**, and **8** are presented in Figures 6–8. Important structural details are given in Table III. Both **6** and **7** have been described in a preliminary communication,[8] but **7** is reproduced here owing to its significant deviation from linearity. A noteworthy feature of the crystals of **5–7** is that they are isomorphous. This is suggestive of very similar structures and indeed, with the exception of more bent nature of **7**, the structures have many features in common. All four compounds are monomeric, essentially two-coordinate, with minor (9–12°) deviations from linearity of the N–M–N moiety in the case of **5**, **6**, and **8**. However, the N–Co–N angle in **7** is 147.0 (1)°. The next closest atoms to cobalt are ca. 2.58 Å distant, and these are carbon atoms C(7) and C(27) each from a phenyl ring. However, there is no apparent lengthening of any bond(s) within the ligand a result of nonbonding interactions with the metal. Instead, the interactions are reflected in the asymmetry in the M–N–Si angles for cobalt and more minor angular distortions in the case of the other complexes. The M–N distances decrease in the order Mn–N > Fe–N > Co–N. It is also notable that the Fe–N distances in **8** are only slightly shorter than those in **6**.

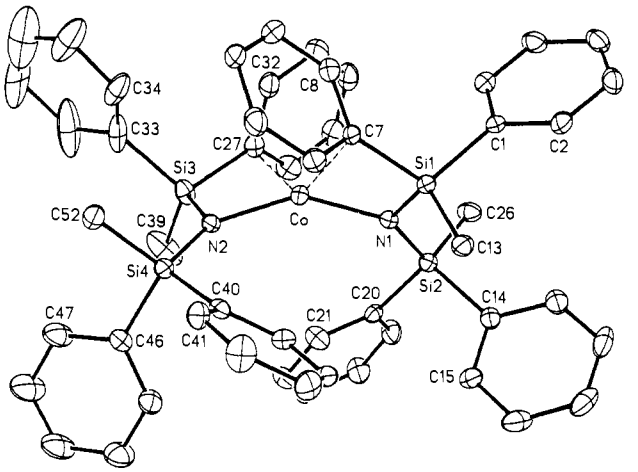

Figure 7. Computer-generated drawing of **7**. Hydrogen atoms omitted for clarity.

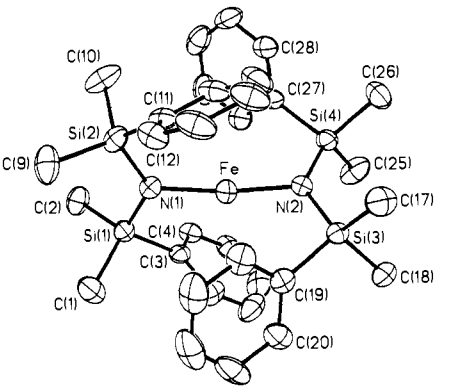

Figure 8. Computer-generated drawing of **8**. Hydrogen atoms omitted for clarity.

Table IV. Isotropic Chemical Shift Data for **6–8** at 300 K in C_7D_8

		Si–Ph		
	Si–Me	o[a]	p	m[a]
$Fe[N(SiMe_2Ph)_2]_2$, **8**	49.9	−88.4	−34.75	−33.9
$Fe[N(SiMePh_2)_2]_2$, **6**	57.6	−35.3	−17.1	−18.8
$Co[N(SiMePh_2)_2]_2$, **7**	50.3	−56.0	−22.7	−26.3

[a] The ortho and meta assignments are only based on comparison with other systems and could be reversed.

^1H NMR Data. The complexes **5–8** are paramagnetic, and their resonances are isotropically shifted. The chemical shift data and assignments for the complexes **6–8** are given in Table IV. No paramagnetically shifted peaks were observed for the manganese complex **5**. Presumably, this is due to the broadness of these resonances. For the iron and cobalt complexes the assignments given in Table IV are relatively straightforward and follow, in

(20) Power, P. P.; Xiaojie, X. *J. Chem. Soc., Chem. Commun.* **1984**, 358.

the main, from comparative data and the relative signal intensities for the different types of ligand protons. In the case of the two iron complexes **6** and **8**, replacement of $-N(SiMePh_2)_2$ by $-N(SiMe_2Ph)_2$ provides additional confirmation of the assignments as a result of the change in the relative intensity of the Me and Ph groups. A variable temperature ^1H NMR study of **7** is also provided. This study was undertaken to establish the temperature coefficients of the paramagnetic peaks and also to detect any difference between the two phenyl rings on the silyl groups that might result from possible Co···C interactions.

Electronic Absorption and EPR Spectra. Electronic spectra were measured in hexane on the complexes **5–8**. However, the complexes **5**, **6**, and **8** were observed to have essentially featureless spectra with an increase in intensity toward the short wavelength. This is consistent with their pale coloration. For the green complex $Co[N(SiMePh_2)_2]_2$, **7**, three bands were observed at 19 010 (ϵ = 70), 15 770 (ϵ = 125), and 12 470 cm^{-1} (ϵ = 50). If a two-coordinate geometry is assumed in hexane solution, then these bands can be assigned to the $^4\Sigma g \rightarrow {}^4\Pi(P)$, $^4\Sigma g \rightarrow {}^4\Sigma g(P)$, and $^4\Sigma g \rightarrow {}^4\Delta\Sigma g(F)$ transitions. Three bands were also reported for $Co[N(SiMe_3)_2]_2$[21] although these appear at 24 400, 17 100, and 14 600 cm^{-1}. Closer agreement between the spectrum of **7** and the solid-state data for $Co[N(SiMe_3)_2]_2$ was found. It is known that $Co[N(SiMe_3)_2]_2$ is three-coordinate at cobalt in the crystalline phase.[22] Thus, it is clear that the UV–vis data are not a reliable guide to the structures of these species. Although the three bands observed for **7** are consistent with a linear structure, they could also be rationalized on the basis of a bent (C_{2v}) or an approximately trigonal coordination as seen in the dimeric $Co[N(SiMe_3)_2]_2$ species.

The EPR spectra of **5–8** were recorded on crystalline samples between 7.6 and 9 K with a typical scan range of $3–5 \times 10^3$ G. The spectrum of the cobalt complex **7** consists of absorptions at g values of 4.27 and 2.11. Both iron complexes display similar patterns. Thus, **6** has absorptions at 9.14 and 2.03 g, whereas **8** has absorptions at 8.67 and 2.08 g. The data for the iron species should, however, be treated with caution. Thus, although strict precautions were taken to exclude air, it is known that EPR spectra of Fe(II) species (difficult to observe due to the absence of the Kramers' degeneracy) have often been erroneously assigned owing to the presence of Fe(III) contaminants. The EPR spectrum of **5** is characterized by a multiplicity of absorptions. There are two major features centered near g values of 7.04 and 2.09, and these peaks are split further. There is also a peak at 1.46 g. This data suggests a considerable number of low-lying energy states in this manganese system.

Magnetic Measurements. There were carried out in C_6H_6/C_6D_6 solution at ambient temperature by using the Evans method.[23] The shifts were measured relative to the residual C_6H_6 resonance. Samples typically involved a concentration of 0.3–0.35 g of **5**, **6**, or **7** in 5 mL of solvent. At 300 MHz differences of 400–750 Hz were observed between the paramagnetically shifted and normal peaks. The measured values of μ (Bohr magnetons) at 296 K for **5** was 5.72; **6**, 5.07; and **7**, 4.42.

Discussion

The functional role played by sterically crowding ligands in achieving low coordination numbers has been recognized for a long time.[2] For example, in the transition metals and lanthanides, the bulky isoelectronic ligands $-N(SiMe_3)_2$ and $-CH(SiMe_3)_2$ have been found to be particularly applicable to the synthesis of stable three-coordinate crystalline compounds.[2b,24] In fact, in the case of the $-N(SiMe_3)_2$ ligand there is now a substantial body of evidence to show that it approaches but does not quite reach the required size to allow two-coordination in open-shell transition-metal complexes in the solid state. For example electron diffraction data[25] on the vapors of the compounds $M[N(SiMe_3)_2]_2$ (M = Mn, Fe, or Co) and also $Mn[CH(SiMe_3)_2]_2$[26] show that they possess a linear structure similar to that of $Zn[N(SiMe_3)_2]_2$.[27] These results have provided conclusive proof of earlier observations regarding the low boiling points of $M[N(SiMe_3)_2]_2$ (M = Mn, Co, or Ni)[3,4] and cryoscopic molecular weight data[21] on $Co[N(SiMe_3)_2]_2$ in cyclohexane that indicated monomeric structures in these phases. However, other data have provided clear evidence of coordinative unsaturation in the $M[N(SiMe_3)_2]_2$ systems. The crystal structures of the bivalent Mn,[28,22] Fe,[29] and Co[22] derivatives show that they are all dimeric in the solid with amide bridges. In addition they readily form adducts with donor solvents. Thus, both Mn[30] and $Fe[N(SiMe_3)_2]_2$[29] from 1:1 adducts with THF that can be distilled without decomposition under a pressure of ca. 0.1 mmHg. The primary objective of the work described in this paper was to develop simple, easily synthesized ligands that would allow ready isolation of crystalline, two-coordinate open-shell (d^1–d^9) transition-metal complexes.[31] The only prior examples of the class of compound that had been structurally characterized involved MnR_2 (R = $C(SiMe_3)_3$[9] or CH_2t-Bu)[10] and the ion NiO_2^{2-} [32] It was possible, at least in theory, to use ligands other than amides to achieve this objective. However, silylamides were selected owing to the combination of their high M–N bond strength, high steric requirements, and ease of preparation. Thus, although bulky alkyls allow the synthesis of the stable two-coordinate manganese(II) complexes MnR_2, R = $-C(SiMe_3)_3$,[9] $-CH_2t$-Bu,[10] and $-CH(SiMe_3)_2$,[26] they have not yet been proven capable of giving similar complexes for other divalent transition metals. In addition, in spite of the advantages inherent in strong M–O bonds, finding alkoxide or aryloxide ligands sufficiently large to stabilize two-coordination has proved difficult owing to the presence of only one organic group on the oxygen atom. A further goal was to combine their precursors, the lithium silylamides, with lithium-sequestering agents to obtain free amide anions which were previously unknown.

Precursor Silylamines and Lithium Derivatives. The bulky silylamine precursors selected were $HN(SiMe_2Ph)_2$, $HN(SiMePh_2)_2$, and $HN(SiPh_3)_2$. Attention was initially concentrated on the latter two species due to their larger size and crystallinity. Their high steric requirements are evident from their structures that show NSiN angles (Table I) that are somewhat wider than those seen in $HN(SiH_3)_2$ and $HN(SiMe_3)_2$. There is, however, no concomitant increase in the N–Si distances suggesting little change in the strength of the Si–N bond. However, it is notable that, as large as these arylsilyl groups are, they are not nearly as sterically demanding as the $-Si(t\text{-Bu})_3$ group which has been shown to induce the remarkably high NSiN angles of 167 (2)° in the compound $HN[Si(t\text{-Bu})_3]_2$.[19]

Both $HN(SiMePh_2)_2$ and $HN(SiPh_3)_2$ are readily deprotonated by n-BuLi in THF or ether/hexane mixtures. It was found to be more convenient (from the crystallographic point of view) to crystallize their solvated lithium derivatives as THF adducts. The structures of both **1** and **2** proved to be monomeric with tricoordinate lithium bonded to two THF's and the disilylamide group. This is in sharp contrast to the dimeric structure of $[Li(Et_2O)N(SiMe_3)_2]_2$ involving four-coordinate nitrogen centers.[33] The

(21) Bradley, D. C.; Fisher, K. J. *J. Am. Chem. Soc.* **1971**, *93*, 2058.
(22) Murray, B. D.; Power, P. P. *Inorg. Chem.* **1984**, *23*, 4584.
(23) Evans, D. F. *J. Chem. Soc.* **1959**, 2005.
(24) The most recent example for $-CH(SiMe_3)_2$ is in the following: Hitchcock, P. B.; Lappert, M. F.; Smith, R. G.; Bartlett, R. A.; Power, P. P. *J. Chem. Soc., Chem. Commun.* **1988**, 1007.
(25) Andersen, R. A.; Faegri, K.; Green, J. C.; Haaland, A.; Lappert, M. F.; Leung, W.-P.; Rypdal, K. *Inorg. Chem.* **1988**, *27*, 1782.
(26) Andersen, R. A.; Haaland, A.; Lappert, M. F. and co-workers, unpublished results.
(27) Haaland, A.; Hedberg, K.; Power, P. P. *Inorg. Chem.* **1984**, *23*, 1972.
(28) Bradley, D. C.; Hursthouse, M. B.; Malik, K. M. A.; Moseler, R. *Transition Met. Chem. (Weinheim, Ger.)* **1978**, *3*, 253.
(29) Bartlett, R. A.; Olmstead, M. M.; Power, P. P.; Shoner, S., unpublished results.
(30) Illustrated in ref 2c. Other adducts are also known, for example, $(PPh_3)Co[N(SiMe_3)_2]_2$ in the following: Bradley, D. C.; Hursthouse, M. B.; Smallwood, R. J.; Welch, A. J. *J. Chem. Soc., Chem. Commun.* **1972**, 872.
(31) Power, P. P. *Comments Inorg. Chem.* **1989**, *8*, 177.
(32) Nowitzki, B.; Hoppe, R. *Croat. Chem. Acta* **1984**, *57*, 537. Hitchman, M. A.; Stratmeier, H.; Hoppe, R. *Inorg. Chem.* **1988**, *27*, 2506.
(33) Lappert, M. F.; Slade, M. J.; Singh, A.; Atwood, J. L.; Rogers, R. D.; Shakir, R. *J. Am. Chem. Soc.* **1983**, *105*, 302. Engelhardt, L. M.; May, A. S.; Raston, C. L.; White, A. L. *J. Chem. Soc., Dalton Trans.* **1983**, 1671.

lack of aggregation in **1** and **2** is due mainly to the larger size of the silyl substituents. However, there are two other interesting features in both structures. These are (a) the shortened N–Si bonds and (b) the wider Si–N–Si angles in comparison to their respective precursors. The N–Si bonds in **1** and **2** are 1.671 (1) and 1.666 (1) Å long and are about 0.05 Å shorter than the same bonds in the precursors. Similarly the N–Si–N angle is slightly increased from 131.6 (1) to 132.3 (1)° in **1** and from 136.1 (2) to 140.5 (2)° in the case of **2**. The increase in ionic bonding, consistent with a greater degree of negative charge on nitrogen, results in a N–Si bond contraction. The N–Si bond shortening can also be accounted for in terms of an increased N–Si, p-dπ interaction as a result of the greater available electron density at nitrogen. These observations are in agreement with the data for the more ionic sodium and potassium $-N(SiMe_3)_2$ derivatives, $NaN(SiMe_3)_2$[34] $K(dioxane)_2N(SiMe_3)_2$,[35] where wide SiNSi angles and shortened N–Si bonds were also seen. A further interesting feature of the structure of **2** is that the Li–N bond is significantly (0.05 Å) longer than that in **1** which is consistent with the larger steric requirements of the $-SiPh_3$ group. In this regard it could also be claimed that the $-SiPh_3$ substituents are more effective than the alkyl silyls in delocalizing the negative charge from the nitrogen center which would lead to the longer Li–N distances. This weakening of the Li–N interaction is apparently just sufficient to enable its rupture upon treatment with 12-crown-4, whereas the shorter Li–N bond in **1** cannot be cleaved under the same conditions.

These trends suggested that it might be possible to achieve complete Li^+ separation if the appropriate complexing agent were added[36] thereby allowing the first structural characterization of a free amide $[NR_2]^-$ anion. Previous attempts to obtain such ions by using 12-crown-4[36] and $LiN(SiMe_3)_2$[20] or $LiNPh_2$[37] had resulted in the isolation of the 1:1 adduct 12-crown-4·$LiNR_2$ (R = Ph or $SiMe_3$) but not Li^+ ion separation. For **1** it was found that addition of excess 12-crown-4 to a solution of $LiN(SiMePh_2)_2$ only resulted in **3** which was a similar 1:1 adduct to those previously described.[20,37] Inspection of the data in Table II shows that the structural parameters for the $-N(SiMePh_2)_2$ moiety are very similar in **1** and **3**. The Li–N and Li–O distances in **3** are, however, significantly longer due to the higher coordination number (5) of lithium in this complex. The addition of 2 equiv of 12-crown-4 to a THF solution of $LiN(SiPh_3)_2$ nevertheless achieved the desired object of ionic separation as illustrated in Figure 5. The Li^+ ion is in the now familiar sandwich complex with two 12-crown-4 molecules.[36] The anion $[N(SiPh_3)_2]^-$ has no close interactions with any other species. Its most notable features are the NSiN angle of 154.9 (3)° and the short NSi bonds of length 1.633 (4) and 1.634 (4) Å. These data may be interpreted in a number of ways. First, by analogy with the isoelectronic PPN^+ cations,[38] it can be argued that the SiN bonds have considerable multiple character as a result of a (p-d) π N–Si bonding. In fact, the N–Si bond lengths are closer to the value reported[39] for an N–Si double bond 1.569 (3) Å than are the values (1.72–1.73 Å) reported for the amine precursors. The short N–Si bonds may also be accounted for in terms of rehybridization or the greatly increased ionic contribution to the bond strength as a result of Li^+ ion separation. As already noted $[Ph_3SiNSiPh_3]^-$ is isoelectronic to $[Ph_3PNPPh_3]^+$. The latter can adopt a large range (ca. 135°–180°) of PNP angles[40] so it was expected that $[Ph_3SiNSiPh_3]^-$ would adopt a similar variety of angles if crystallized with the appropriate cations. An increasing SiNSi angle corresponds to a greater p character in the two nitrogen lone-pair orbitals and hence more effective p-d π overlap. This should give shorter Si–N bonds lengths close to the value for the N=Si double bond. A linear arrangement has already been observed in the closely related $Ph_3SiOSiPh_3$ molecule.[41] A further result of the wider SiNSi angles should be a decreasing availability of the lone-pair electrons on nitrogen as a result of their more effective interaction with the Si d-orbitals. Supporting evidence for this view comes from the reaction of $LiN(SiPh_3)_2$ with transition-metal dihalides which has so far failed to give characterizable complexes. The amine $HN(SiPh_3)_2$ can usually be isolated from these reaction mixtures. This apparent reluctance to form complexes may also be rationalized from steric and electronic considerations in which the very large $SiPh_3$ substituents discourage complexation by the $N(SiPh_3)_2$ ligand.

Two-Coordinate Transition-Metal Silylamides 5–8. The reaction between $LiN(SiMePh_2)_2$ (2 equiv) and MnI_2, $FeBr_2$, or $CoCl_2$ in Et_2O or THF solution gave crystalline complexes in good yield. X-ray data indicate that the respective products **5**, **6**, and **7** are all monomeric. This in contrast to the data for the $-N(SiMe_3)_2$ derivatives which are all dimeric in the solid state with amide bridges. The ligand $-N(SiMe_2Ph)_2$ also leads to a monomeric complex in the solid as exemplified by the iron derivative **8**. The monomeric nature of these four complexes is, in the main, due to steric effects. Thus, neither **5**, **6**, nor **7** form strong adducts with THF, whereas species such as $[(THF)M[N(SiMe_3)_2]_2]$ (M = Mn or Fe) may be distilled without decomposition.[29,30]

A significant feature of the structures **5–8** is their deviation from linearity. This is in contrast to the vapor-phase structures of the species $M[N(SiMe_3)_2]_2$ (M = Mn, Fe, or Co) which reveal them to have a linear N–M–N moiety.[25] However, the deviations from linearity are slight in the case of **5**, **6**, and **8** which all possess N–M–N angles near 170°. Inspection of the data in Table III shows that next nearest neighbor to the metals is a carbon atom from a substituent phenyl ring or rings. Not surprisingly, the shortest M···C distances are associated with the more distorted cobalt center. An apparent manifestation of the close M···C approaches involves an asymmetry in the M–N–Si bond angles which was observed in all four complexes (see Table III for details). The magnitude and extent of the MNSi bond angle asymmetry corresponds roughly to the closeness of the approach of the carbon(s) in all cases. For example, the weakest interactions are in species **5** and **6** where the closest approaches are 2.774 (5) and 2.695 (4) Å involving the carbon atoms C(7) and C(14), respectively. The next closest carbons are at 2.95–2.97 Å. In both cases these weak interactions are reflected in asymmetry in the MN(1)Si(1) and MN(1)Si(2) angles of 13° and 14.8°, whereas there is only negligible asymmetry in the angles at the N(2) ligand center for both complexes which involves no M···C interactions. For the cobalt complex **7**, however, M···C interactions (~2.586 Å) are seen for both the N(1) and N(2) amide groups and the amount of asymmetry (~27°) is the same at both N(1) and N(2). Minor (5.7°) distortions in the FeNSi angles are also evident in the complex **8** with the closest FeC approach being 2.633 Å. The latter result indicates that the angular distortions are also closely related to the size of the ligands. There is, however, little change in the N–Si bond lengths throughout the complexes **5–8**. In fact, the distances are quite close to those observed in the corresponding metal $-N(SiMe_3)_2$ derivatives. In view of this and the weak M···C ligand interactions in **5–8** it is probable that both the NMN and NSi_2 angles are relatively easily distorted and that bending in **5–8** could be due to packing forces.

The metal–nitrogen bond distances also merit comment. The values in Table III (from X-ray data at 130 K) are about 0.05 Å longer than those measured for the monomers $M[N(SiMe_3)_2]_2$ (M = Mn, Fe, Co), by electron diffraction at ca. 320 K.[25] The M–N distances in **5–8** are in fact quite close to the M–N (terminal) distances observed in the dimers $[M\{N(SiMe_3)_2\}_2]_2$[22,31] (M = Mn, Fe, Co). The agreement between the M–N (terminal) values in the solid are thus at variance with the shorter M–N values (Table III) from electron diffraction.[25] One possible explanation is that longer distances are expected in the compounds

(34) Grüning, R.; Atwood, J. L. *J. Organomet. Chem.* **1977**, *137*, 101.
(35) Domingos, A. M.; Sheldrick, G. M. *Acta Crystallogr. Sect. B* **1974**, *305*, 517.
(36) Power, P. P. *Acc. Chem. Res.* **1988**, *21*, 147.
(37) Bartlett, R. A.; Dias, H. V. R.; Hope, H.; Murray, B. D.; Olmstead, M. M.; Power, P. P. *J. Am. Chem. Soc.* **1986**, *108*, 6921.
(38) Appel, R.; Hauss, A. *Z. Anorg. Allg. Chem.* **1961**, *311*, 291.
(39) Wiberg, N.; Schurz, K.; Reber, G.; Müller, G. *J. Chem. Soc., Chem. Commun.* **1986**, 591.
(40) Wilson, R. D.; Bau, R. *J. Am. Chem. Soc.* **1974**, *96*, 7601.
(41) Glidewell, C.; Liles, D. C. *J. Chem. Soc., Chem. Commun.* **1977**, 632.

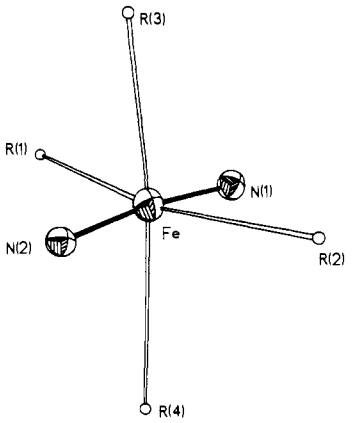

Figure 9. Drawing of **8** illustrating the pseudooctahedral coordination arising from the geometry at the iron atom in the amide ligands and phenyl group.

5–8 because of the bulkier substituents. In addition the terminal M–N distances in the dimers $[M\{N(SiMe_3)_2\}_2]_2$ are expected to be longer because of the three-coordinate nature of the metal centers. However, there is little evidence of severe steric strain within the ligands in **5–8**. In addition, the dimerization in the species $[M\{N(SiMe_3)_2\}_2]_2$ is weak and unlikely to give rise to substantial lengthening in the terminal M–N bonds. It is also notable that in the iron complexes **6** and **8**, the Fe–N distances (involving the ligands $-N(SiMePh_2)_2$ and $-N(SiMe_2Ph)_2$) only differ by 0.014 Å. These data indicate that although some further shortening is expected in the less crowded $Fe[N(SiMe_3)_2]_2$ monomer, it is unlikely that is would be large enough to lead to a value of 1.84 Å for the Fe–N bond. Another possible explanation is that a low spin configuration for $Fe[N(SiMe_3)_2]_2$ could lead to short Fe–N bonds. However, magnetic studies on **6** (vide infra) indicate that it has a high spin configuration suggesting the same configuration for $Fe[N(SiMe_3)_2]_2$. Indeed, currently available magnetic data on the solid $[Fe\{N(SiMe_3)_2\}_2]_2$ indicate that the iron centers in this species are high spin.[25] A more plausible explanation for the discrepancy in the M–N distances derives from a source inherent in the electron diffraction data. The authors point out that there is a strong correlation between the M–N bonds and the similar Si–C bond distances.[25] This results in a reduced reliability in the M–N bond lengths and could give rise to the observed variance.

Several further observations regarding the structures of **5–8** may be made (i) As a result of their essentially two-coordinate structures the complexes probably have a tendency to distort owing to the very low number of electrons in the valence shell. There are theoretical and photoelectron spectral data[26] which support a rather ionic picture of the M–N bonds and the treatment of an amide groups as an essentially one-electron ligand. Accordingly, **5**, **6**, and **7** possess 9, 10, and 11 electrons in their valence shells and presumably a predisposition to increase the number by interacting with any available electron rich groups such as phenyl rings. (ii) The distortions in **5**, **6**, and **8** are quite small and probably involve only a few kilocalories (probably 5 or less) of energy. This conclusion is based upon ^1H NMR data (vide infra), the long M···C interactions, and a lack of any measureable distortions of bond lengths within or near the phenyl groups closest to the metals. (iii) The size of the metals decreases in the order Mn(II) > Fe(II) > Co(II). Thus, on the basis of steric arguments it is expected that the widest N–M–N angle would be found for the cobalt complex **7**. However, the lowest NMN angle 147.0 (1)° is observed in this case. This finding may be partly accounted for on the basis of the stability of a pseudotetrahedral structure for **7** which is a d^7 ion. The d^7 electron configuration offers one of the most favorable CFSE energies for the tetrahedral geometry of any of the transition-metal ions. (iv) It is the presence of phenyl rings on the silyl groups which prevents association of the monomeric two-coordinated species by blocking access to the metal centers. This phenomenon is well illustrated in the structure of

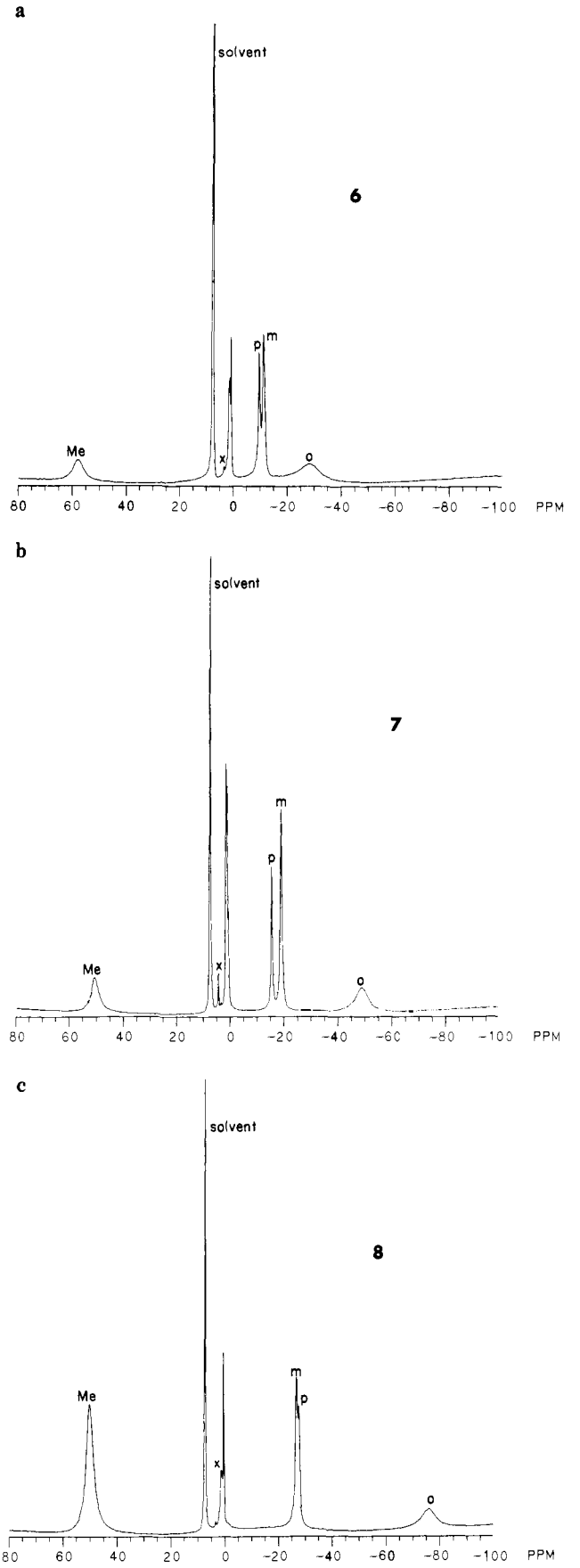

Figure 10. ^1H NMR spectra of **6**, **7**, and **8** in C_6D_6.

8, Figure 8, in which the four phenyl groups are observed to surround the metal. Furthermore, if imaginary lines are drawn between the metal to the centroids of the benzene rings, an ap-

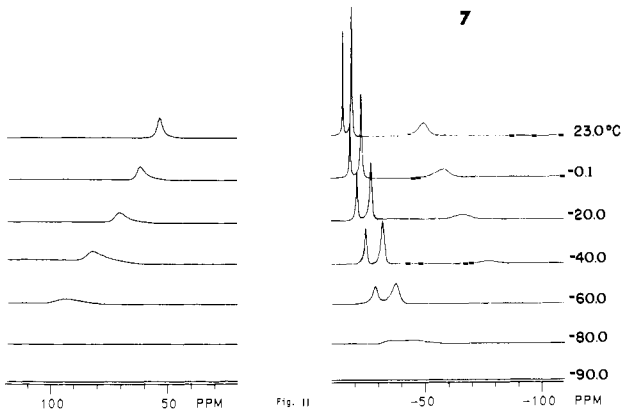

Figure 11. Variable temperature ^1H NMR spectrum of the anisotropically shifted peaks of **7** in C_7D_8.

proximately octahedral configuration results as illustrated in Figure 9. Therefore, the four phenyls serve as a very effective shield of the metal center from attack by all but the smallest molecules.

^1H NMR of 6–8. The solution ^1H NMR spectra of **5–8** were also recorded in C_6D_6 or C_7D_8. No paramagnetically shifted peaks were observed for **5** due presumably to the broadness of the resonances. It is well-known that the ^1H NMR spectra of Mn(II) complexes are often difficult to observe as a result of slow electron exchange which, through fluctuating magnetic fields, causes rapid relaxation between the ^1H NMR energy levels. In the case of **6–8** only one set of peaks was observed for the Ph groups even in the low-temperature spectrum of **7**.

The magnetic interactions affording the isotropically shifted spectra of compounds **6–8** may be recognized from the table of shift data involving $(\Delta H/H_o)_{iso} = (\Delta H/H_o)_{contact} + (\Delta H/H_o)_{dipolar}$ in Table IV and spectra illustrated in Figures 10 and 11. The data for the iron and cobalt complexes $M[N(SiMePh_2)_2]_2$ are similar to each other, Figure 10. It is notable that the shifts of the peaks due to the meta and para hydrogens alternate in the two complexes. In addition, the ortho peak appears at a very different chemical shift in the three complexes. Thus, for the phenyl groups, the shifts are not just dependent on their distance from the paramagnetic center. This observation suggests that these shifts are mainly a result of contact interactions although dipolar interactions may also contribute significantly. The methyl resonances exhibit negative temperature coefficients of isotropic shift in the range −90° to 23 °C. This behavior is approximately parallel to that expected for $\chi_M(T)$ by the Curie–Weiss law and is consistent with, but does not necessarily prove, mainly contact interaction. The variable temperature ^1H NMR study of the cobalt complex **7**, Figure 11, study also served as a probe of any possible M···C interactions. However, even in this case where the closest M···C interactions were observed in the solid, no differences in the phenyl resonances could be observed to a temperature of −90 °C. This suggests that any possible M···C interactions in solution are probably either nonexistent or extremely weak.

The assignment of peaks in the spectra of **6–8** is also worthy of comment. For all complexes the Si–Me proton resonances have been assigned as the downfield peak. There are a number of reasons for believing that this assignment is correct. The main one is the increase in the relative intensity of this peak between the complexes **6** and **8** and the decrease in the relative intensity of the phenyl peaks between **6** and **8**. Further support for the downfield methyl assignment comes from the ^1H NMR spectrum of $Fe[N(SiMe_3)_2]_2$ in C_6D_6 which displays a broad singlet at 65 ppm[42] close to the assigned values in **6** and **8**. Assignment of the para phenyl peaks was made on the basis of relative peak intensities within each compound. The assignments of the ortho and meta resonances, however, are not unambiguous but are at least consistent in the three compounds. The agreement between the relative intensity data for the various proton types within each spectrum is not, however, quite as clear cut as the difference seen between the two compounds **6** and **8**. The sole reason for the assignments given is based on comparison with other systems[43] having ligand phenyl substituents in which the meta protons are often observed at shifts quite disparate (also frequently opposite in sign) from the ortho resonances. Nevertheless, the ortho and meta peaks could be reversed, and an unambiguous assignment awaits the preparation of species with different substituents at these ring positions.

Application of the Evans method[23] allowed the determination of the number of impaired electrons in **5**, **6**, and **7**. Measurement of the magnetic moment, μ, of each complex afforded the values 5.72, 5.07, and 4.42 Bohr magnetons for **5**, **6**, and **7** at 300 K.[44] These values indicate the presence of 5, 4, and 3 unpaired electrons for the Mn, Fe, and Co complexes. In other words the complexes are all high spin. This result is expected in view of the low number of ligands, and, in addition, data on the metal trisilylamides have shown that they are high spin in all cases. The results are also in agreement with the prediction of a high spin configuration for $Mn[N(SiMe_3)_2]_2$.[25] However, the possibility of a low spin configuration for $Fe[N(SiMe_3)_2]_2$ to account for its unusually short (1.84 Å) Fe–N bond distance[25] is not supported by the observed high spin configuration of $Fe[N(SiMePh_2)_2]_2$ which as Table III shows has an average Fe–N distance of 1.917 (2) Å. However, it is notable that **8** has a somewhat shorter Fe–N distance of 1.903 (2) Å suggesting a shortening trend might be expected in $Fe[N(SiMe_3)_2]_2$.

In summary, the readily accessible ligands $-N(SiMe_2Ph)_2$ and $-N(SiMePh_2)_2$ have been shown to be capable of stabilizing two coordination in the solid state for the metals Mn, Fe, and Co. The large size of these ligands is also underlined by the monomeric structures observed for the THF solvates of their lithium salts. In the extreme case of $-N(SiPh_3)_2$ the substituents are so large that ligand behavior toward the transition metals is not observed. However, this enables the unique $[Ph_3SiNSiPh_3]^-$ ion to be readily isolated.

Acknowledgment. We thank the donors of the Petroleum Research Fund, administered by the American Chemical Society, for financial support.

Supplementary Material Available: Tables of crystallographic data, summary of data collection and refinement, positional parameters for non-hydrogen atoms, bond distances and angles, anisotropic thermal parameters and hydrogen coordinates (28 pages). Ordering information is given on any current masthead page.

(42) Chen, H.; Shoner, S. C.; Power, P. P., unpublished work.
(43) Sigel, G. A.; Bartlett, R. A.; Decker, D. A.; Olmstead, M. M.; Power, P. P. *Inorg. Chem.* **1987**, *26*, 1773.
(44) This result has now been confirmed by magnetic measurements on the solids: Andersen, R. A., personal communication.